Supporting Information

METHODS

Animals

All mouse strains were in C57BL/6J background. Animals of both sexes were used. WT C57BL/6J mice were purchased from Jackson Laboratories. The astrocyte-specific Cx43 KO mouse line ($Cx43^{aKO}$) was established in house using the Cre-loxP recombination system. Mice with floxed *Cx43* gene ($Cx43^{flox}$) (Stock number 008039, The Jackson Laboratory) were crossed with mGFAP-Cre expressing mice (Stock number 012886, The Jackson Laboratory). The heterozygous ($Cx43^{aKO/flox}$) mice were backcrossed with $Cx43^{flox}$ mice, to generate WT ($Cx43^{flox}$), heterozygous ($Cx43^{aKO/flox}$) and homozygous astrocyte-specific KO ($Cx43^{aKO}$) mice. Expression of Cre recombinase in astrocytes was confirmed by crossing GFAP-Cre mice with loxP-tdTomato Ai9 reporter mice (Stock number 007909, The Jackson Laboratory). The endothelial cell-specific Cx43 KO mouse line ($Cx43^{eKO}$) was established following the same strategy using mTie2-Cre expressing mice (Stock number 008863, The Jackson Laboratory). Site-specific phosphorylation-deficient knockin mice in which the serines 325 and 330 have been replaced with alanines, and the serine 328 has been replaced with tyrosine (S325A/S328Y/S330A referred to as $Cx43^{S3A}$) were generated previously (57). All animal procedures were conducted in accordance with Association for Research in Vision and Ophthalmology statement regarding use of animals in vision research and were approved by the SUNY Optometry Institutional Animal Care and Use Committee.

The mouse model of OIR

Mice pups were exposed to 75% oxygen for 5 days, from postnatal day 7 (P7) to P12, as described previously (28-30). Exposure to hyperoxia early in postnatal development (P7-P12) resulted in the disappearance of the capillary network in the central retina. At P12, mice returned to room air until P17. During this period, the central retina became hypoxic because of the absence of capillaries in this region. Hypoxia led to extensive proliferation of vessels and neovascular tuft formation. Partial revascularization of the avascular central retinal area also occurred during this phase. The phenotype observed in the OIR model is strongly influenced by the weight of the neonatal mice (28). All mice weighing less than 6 g at P17 were excluded from the study.

Intravitreal injections

Mice pups were anesthetized with i.p. administration of 50 µg Ketamine/g body weight and 5 µg Xylazine/g body weight diluted in saline. The Cx43 inhibitor SBO15 [compound 18 = 5-(4-phenoxybutoxy) isoquinoline in (42)] and the CK1δ inhibitor PF670462 (Tocris Bioscience) were diluted in PBS. Using a 36-gauge needle, 0.5 µl of the drugs at various concentrations were administered to the vitreous of the left eyes. The right eyes received 0.5 µl PBS to serve as SHAM.

Frozen sections

Eyes were enucleated and retinas were isolated and fixed in paraformaldehyde (PFA) solution (4% in PBS, Santa Cruz Biotechnology) for 30 minutes at room temperature. Retinas were incubated sequentially in 10% and 20% sucrose solution for 2 hours at room temperature and in 30% sucrose

solution overnight at 4°C. Retinas were embedded in tissue freezing media (Electron Microscopy Science), and sliced vertically at 10μm.

Immunohistochemistry

For whole-mount preparations, eyes were enucleated and retinas were isolated and fixed in PFA solution (4% in PBS, Santa Cruz Biotechnology) for 1 hour at room temperature. Tissue was incubated with 5% (v/v) normal goat serum (Thermo Fisher Scientific) and 0.5% (v/v) TritonX (Millipore Sigma) in PBS for 1 hour at room temperature for blocking of non-specific antibody binding and permeabilization, respectively. Whole-mounts and vertical frozen sections were incubated with appropriate primary antibodies overnight at 4°C, washed with PBS and further incubated with fluorescent secondary antibodies for 1 hour at room temperature. Primary antibodies included IsolectinB4 conjugated with Alexa Fluor 488 (Thermo Fisher Scientific, I21411, 1:100) to visualize the vasculature, rabbit anti-Cx43 (Millipore Sigma, C6219, 1:2000), mouse anti-GFAP (Millipore Sigma, MAB360, 1:500), mouse anti-CRALBP (Abcam, ab15051, 1:250) and rabbit anti-Annexin V (Abcam, ab14196, 1:250). Secondary antibodies (1:500) included goat anti-rabbit conjugated with Alexa Fluor 594, goat anti-mouse conjugated with Alexa Fluor 647, donkey anti-mouse conjugated with Texas Red, donkey anti-mouse conjugated with Alexa Fluor 488 and streptavidin conjugated with Alexa Fluor 488 (Thermo Fisher Scientific). Upon staining, samples were mounted to glass slides using mounting medium with DAPI (Vectashield, Vector Labs). Imaging was performed using a confocal microscope (Olympus).

Quantification of vaso-obliteration and neovascularization

The retinal vasculature was visualized using Alexa Fluor 488-conjugated IsolectinB4. The retinal areas that remained avascular and the formation of neovascular tufts were quantified as described previously (28). Briefly, confocal microscopy images of each whole-mounted retina were obtained at 4x magnification. Using Photoshop software, the number of pixels in the vaso-obliterated areas and in the neovascular tufts were counted and compared to the number of pixels of the total retinal area.

Quantification of astrocytic density

Retinal whole-mounts were stained for GFAP and Isolectin. Confocal microscopy images were obtained at 20x and 60x magnifications. The avascular area of all quarters of each retinal whole-mount was divided into four non-overlapping, random size rectangular regions (total 16 rectangles for each retina) using Photoshop software. The number of astrocytes was counted manually, normalized to an area of $1mm^2$, and was averaged across regions to obtain an astrocyte number for each retina. Astrocytes were identified as GFAP-expressing cells with DAPI-stained nuclei localized at the level of the superficial vascular plexus (DAPI staining is not shown for clarity purposes). In this layer, GFAP staining of Müller cells corresponds to their end feet and not their cell bodies (located in the INL). Therefore, Müller cells were excluded from the quantification. Astrocytes with cell bodies attached to main veins and arteries were also excluded from analysis.

Fluorescent Hypoxyprobe assay

The hypoxic retinal areas were assessed using Hypoxyprobe (pimonidazole HCl). Mice at P17 exposed to OIR were injected intraperitoneally with Hypoxyprobe (2.5 mg/pup). After 1 hour, animals were euthanized and retinas were fixed and stained with Dylight 546-conjugated anti-

pimonidazole (Hypoxyprobe, HP7-100Kit) and Alexa Fluor 488-conjugated IsolectinB4 antibodies.

Western blot

Retinas were dissected at different time points and homogenized in RIPA lysis buffer (Millipore Sigma) containing 1% protease inhibitor cocktail (Millipore Sigma) and 1% phosphatase inhibitor cocktail (Roche). 20 µg of total retinal protein extract from individual mice were loaded in 10% acrylamide gels for electrophoresis. Separated proteins were transferred to nitrocellulose membranes (GE Healthcare), which were incubated overnight with primary antibodies against Cx43 (Millipore Sigma, C6219, 1:8000), Ser325/328/330-phosphorylated Cx43 (48), CK1δ (Thermo Fisher Scientific, PA5-32129, 1:3000) or tubulin (Millipore Sigma, T6074, 1:10000). Fluorescent secondary antibodies (1:20000) were used for protein detection with an Odyssey imager (LI-COR Biosciences). Cx43 and CK1δ protein levels were normalized to tubulin expression under each condition. Quantitative analysis of protein expression was performed by measuring band intensities using ImageJ software.

ERG recordings and data analysis

Scotopic ERGs were recorded as described previously (58). Four-week old mice were dark adapted for 18-24 hours. Animals were anesthetized with intraperitoneal administration of 70 µg Ketamine/g body weight and 7 µg Xylazine/g body weight diluted in saline. Pupils were dilated with topical phenylephrine hydrochloride solution (2.5%) (Akorn) and tropicamide solution (1%) (Akorn). Topical application of methylcellulose (1%) was used to keep the cornea moist. Body temperature was maintained at 37 ^{o}C with a heating pad. Platinum electrodes were placed at the cornea of both eyes. The reference electrode was inserted into the cheek and the ground electrode was inserted under the back skin. ERG responses to brief white LED test flashes with intensities in the range of -6.7 - 2 log scot. cd.s/m^2 were recorded using the Espion electrodiagnostic system (Diagnosys LLc). Recording periods lasted 60-90 minutes. All mice recovered from anesthesia after sessions. The a-wave amplitudes were measured from baseline to the maximum trough. The b-wave amplitudes were measured at their peak from the b-wave trough. Oscillatory potentials (OPs) in the range of 70-300 Hz were extracted by digital filtering and quantified by summing the peak-to-trough amplitudes of the individual OPs within the first 100 ms. Responses of both eyes to each stimulus intensity were averaged to represent a single data point. A generalized Naka Ruston equation (59) was fit to the data and the maximum response amplitude (V_{max}), the slope (n) and the semisaturation constant (K) were estimated.

Dye coupling

Eyes were enucleated and retinas were dissected in oxygenated HEPES buffer, transferred to filter papers (12 mm diameter cell culture inserts with 0.4 µm pore size, Millipore Sigma) and kept in a chamber perfused with oxygenated bicarbonate extracellular buffer. A single astrocyte from each preparation was identified either based on the cell morphology and localization or based on its red fluorescence when GFAP-tdTomato mice were used. The whole-cell clamped astrocyte was loaded with the GJ permeable tracer Neurobiotin (5 mg/ml) for 15 minutes. Neurobiotin-filled cells were visualized using Alexa Fluor 488-conjugated streptavidin, which binds to Neurobiotin. To ensure that the injected cells are astrocytes, retinas were stained with a mouse-anti GFAP primary antibody followed by donkey anti-mouse secondary antibody conjugated with Texas Red.

Astrocytes labeled with Neurobiotin were counted manually in images obtained with confocal microscopy.

Dye uptake

Eyes were enucleated, retinas were dissected and incubated in PBS in the presence or absence of 300 μM Gap19 (Millipore Sigma) for 15 minutes at room temperature. 4 μM Ethidium Bromide (EtBr) (Millipore Sigma) were added to the solution for 10 minutes. Retinas were rinsed with PBS, fixed with PFA for 30 minutes and stained against GFAP for confocal imaging.

Transient Transfection of Mammalian Cells

HeLa cells were cultured in DMEM (Thermo Fisher Scientific) supplemented with 10% FBS (Thermo Fisher Scientific) and 1% penicillin/streptomycin. Cells were transiently transfected with 500 ng of WT Cx43, Cx43_S325A/S328A/S330A, or WT Cx36 cDNAs in combination with mCherry plasmid (Clontech) with Lipofectamine 2000 reagent (Thermo Fisher Scientific), according to the manufacturer's instructions. DNA concentrations were measured using Nanodrop 2000 (Thermo Fisher Scientific). Cells were plated at low density onto glass coverslips.

Statistics

Normal distributions were confirmed before analyses. Two-sided two-sample Student's t-test at the significance level of $\alpha = 0.05$ (95% confidence interval) was used for comparisons between two mice groups of different genotype and between two different time points. Two-sided one-sample Student's t-test at the significance level of $\alpha = 0.05$ (95% confidence interval) was used for comparisons between retinas that received different injections (SHAM versus SBO15, SHAM versus PF670462). One- and Two-way ANOVA with multiple comparisons correction at the significance level of $\alpha = 0.05$ (95% confidence interval) were used for comparisons between multiple mice groups with or without treatment, and between multiple time points. Statistical analyses were performed using the Graph Pad Prism7 software. Results are presented as mean ± SEM. "N" values correspond to number of mice used in ERG experiments and "n" values correspond to number of retinas used in all other experiments.

Fig. S1

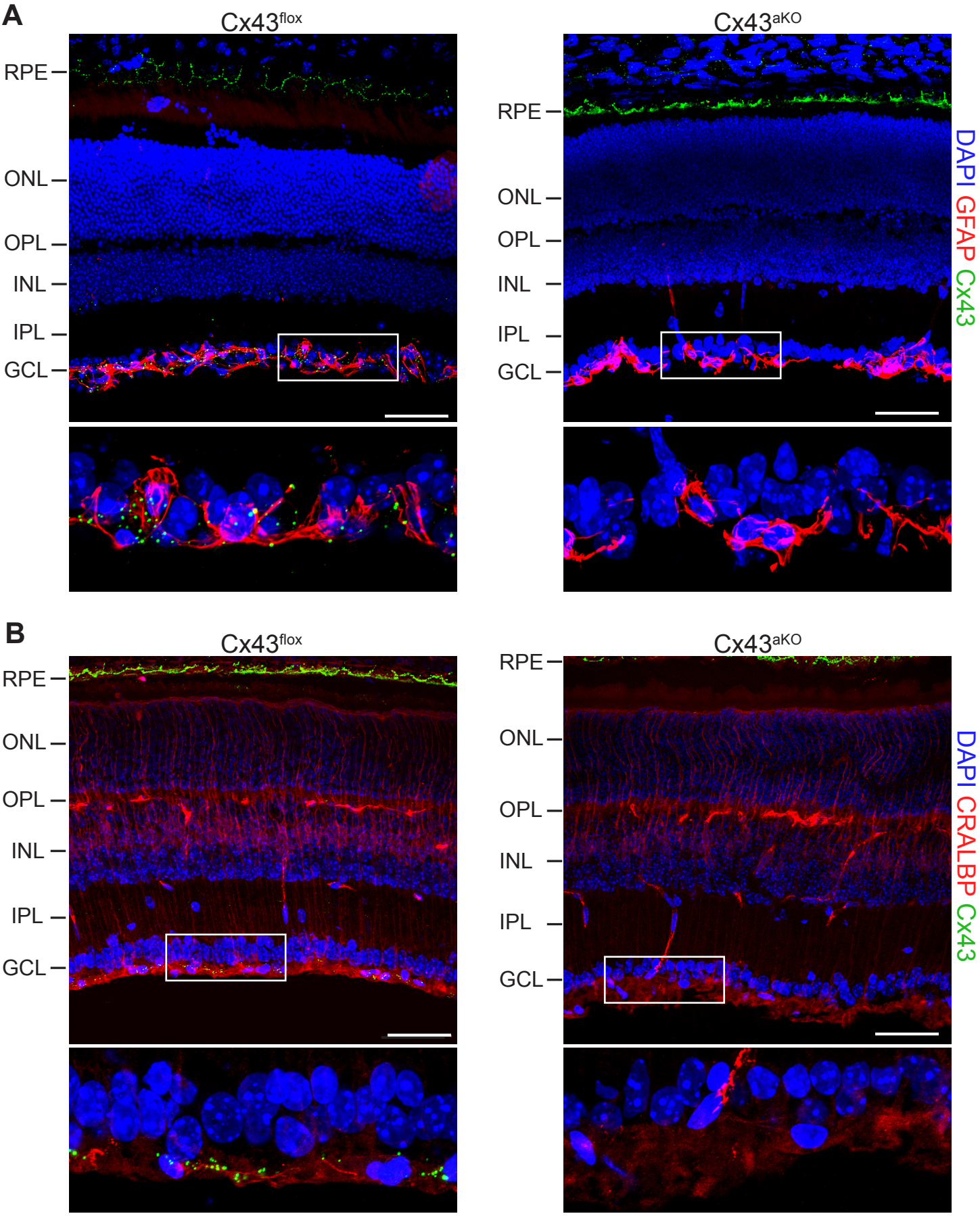
A
Cx43flox
Cx43aKO
RPE
ONL
OPL
INL
IPL
GCL
DAPI GFAP Cx43
B
Cx43flox
Cx43aKO
RPE
ONL
OPL
INL
IPL
GCL
DAPI CRALBP Cx43

Fig. S1: Cx43 expression in vertical retinal sections during early development in normoxic conditions. (**A**) Representative images of vertical retinal sections from $Cx43^{flox}$ and $Cx43^{aKO}$ mice at P13, immunostained with anti-GFAP (red) and anti-Cx43 (green). Nuclei are counterstained with DAPI (blue). Cx43 staining is primarily detected in the GCL and the RPE in $Cx43^{flox}$ retinas. In the GCL, Cx43 co-localizes with GFAP-expressing cells, which are predominantly astrocytes. Müller cells do not express GFAP in normoxic conditions. Glial Cx43 is absent in $Cx43^{aKO}$ retinas, indicating deletion of the protein in astrocytes. (**B**) Representative images of vertical retinal sections from $Cx43^{flox}$ and $Cx43^{aKO}$ mice at P13 immunostained against the Müller cell-specific marker CRALBP (red) and Cx43 (green). Insets show the boxed areas in high magnification. Cx43 expression is found around nuclei (blue) in the GCL of $Cx43^{flox}$ retinas. Cx43 puncta are not observed in Müller cell bodies or processes. No Cx43 is seen in $Cx43^{aKO}$ inner retinas, indicating that staining in $Cx43^{flox}$ retinas corresponds to GFAP- and not CRALBP-expressing cells. Scale bars: 50 μm.

Fig. S2

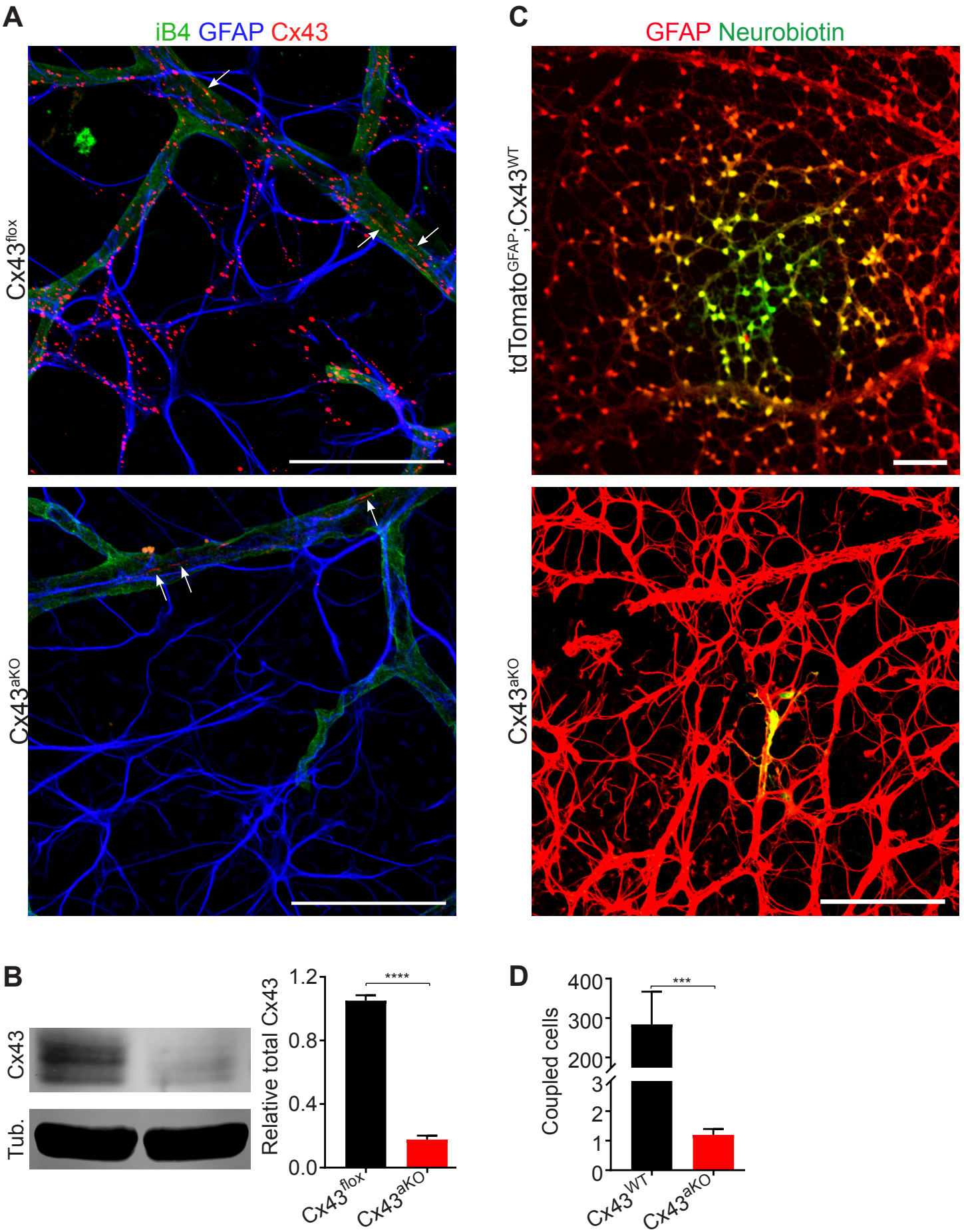
A
iB4 GFAP Cx43
Cx43flox
Cx43aKO
C
GFAP Neurobiotin
tdTomatoGFAP;Cx43WT
Cx43aKO
B
Cx43
Tub.
Relative total Cx43
1.2
0.8
0.4
0.0
****
Cx43flox
Cx43aKO
D
Coupled cells
400
300
200
3
2
1
0
***
Cx43WT
Cx43aKO

Fig. S2: Cx43 expression in retinal whole-mounts during early development in normoxic conditions. (**A**) Representative images of whole-mount normoxic retinas from $Cx43^{flox}$ and $Cx43^{aKO}$ mice at P13. Cx43 (red) co-localizes with GFAP-expressing astrocytes in $Cx43^{flox}$ retinas but is absent in astrocytes of $Cx43^{aKO}$ retinas. Blood vessels are labeled with isolectin B4 (green). Cx43 staining is weakly expressed in the vasculature (arrows). Scale bars: 50 μm. (**B**) Western blot and quantification of total Cx43 in normoxic $Cx43^{flox}$ (n = 7) and $Cx43^{aKO}$ (n = 5) retinas. A large decrease in Cx43 protein levels is found in retinal lysates obtained from $Cx43^{aKO}$ compared to $Cx43^{flox}$, consistent with the expression pattern of Cx43 shown above. (**C**) GJ coupling between astrocytes from $tdTomato^{GFAP}$ ($Cx43^{WT}$) and $Cx43^{aKO}$ retinas was visualized by diffusion of Neurobiotin. Images show streptavidin staining against Neurobiotin (green). Scale bars: 100 μm. (**D**) Quantification of astrocytes labeled with Neurobiotin in $Cx43^{WT}$ (n = 4) and $Cx43^{aKO}$ (n = 3) retinas. Deletion of Cx43 led to a complete reduction in GJ coupling between astrocytes. Data are presented as mean ± SEM. Student's t test, ***P < 0.001, ****P < 0.0001.

Fig. S3

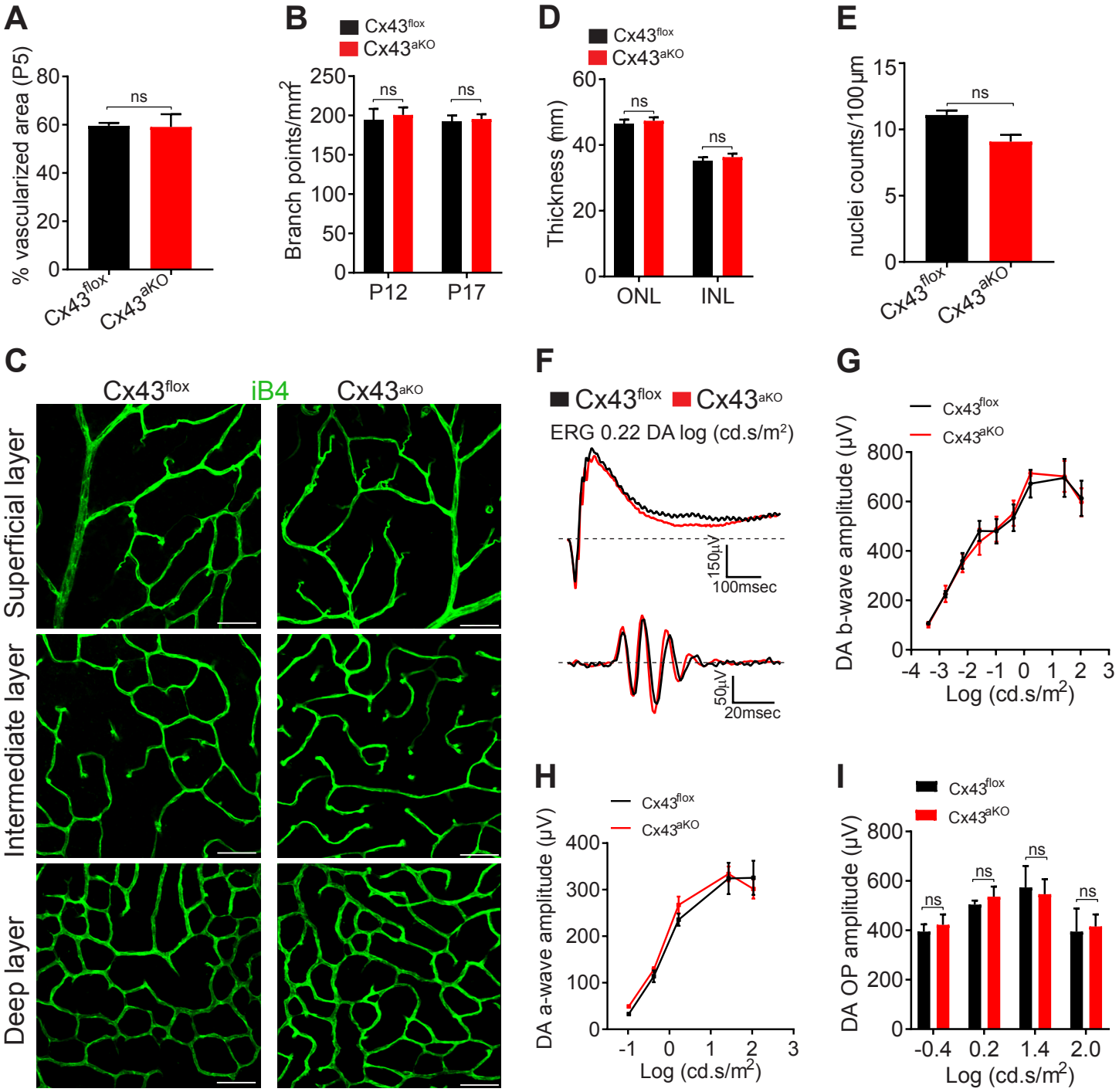

Fig. S3: **Cx43^{aKO} retinas exhibit normal development, structure and function.** (**A**) The retinal areas covered with blood vessels at P5 in Cx43^{flox} and Cx43^{aKO} mice (n = 3-4) showed equal degree of angiogenesis in the two groups. (**B**) The number of branch points in the superficial vascular layer of retinas at P12 (n = 4-6) and at P17 (n = 4-7) was unaffected by deletion of Cx43. (**C**) Isolectin staining of vessels in superficial (*top*), intermediate (*middle*) and deep (*bottom*) layers from normoxic Cx43^{flox} and Cx43^{aKO} whole-mount retinas at P17. The appearance of all three vascular plexuses was similar between the two groups. Scale bars: 50 µm. (**D, E**). The thickness of the ONL and INL, as well as the cell counts per 100 µm length of vertical sections in the GCL were also unaffected (n = 6). (**F**) Representative a- and b-waves (*top*) and OPs (*bottom*) of scotopic ERGs from Cx43^{flox} and Cx43^{aKO} mice at P28. Light intensity = 1.7 scot. cd.s/m^2. (**G-I**) Quantifications of the amplitudes of scotopic b-wave (**G**), a-wave (**H**) and the summed OP (**I**) amplitudes from Cx43^{flox} and Cx43^{aKO} mice at different stimulus intensities (N = 4). Data are represented as mean ± SEM. Student's t test, ns P > 0.05.

Fig. S4

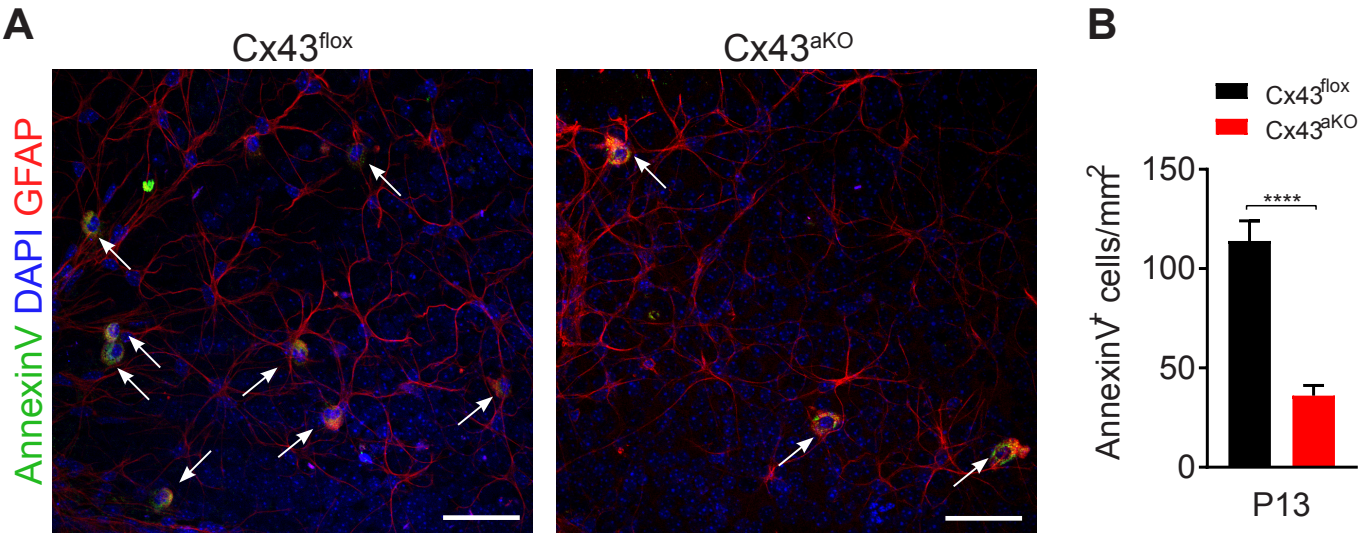

Fig. S4: **Conditional deletion of Cx43 reduces apoptosis of astrocytes in OIR.** (**A**) Representative images of whole-mount OIR retinas from Cx43^{flox} and Cx43^{aKO} mice at P13, immunostained with anti-GFAP (red) and anti-AnnexinV (green). Nuclei are counterstained with DAPI (blue). Arrows indicate AnnexinV-positive/GFAP-positive cells. Scale bars: 50 µm. (**B**) Quantification of AnnexinV-positive/GFAP-positive cells present in the avascular areas of Cx43^{flox} (n = 8) and Cx43^{aKO} (n = 8) retinas in OIR at P13. Deletion of Cx43 led to a decrease in the number of apoptotic astrocytes in the avascular retinal regions compared to control. Data are presented as mean ± SEM. Student's t test, ****P < 0.0001.

Fig. S5

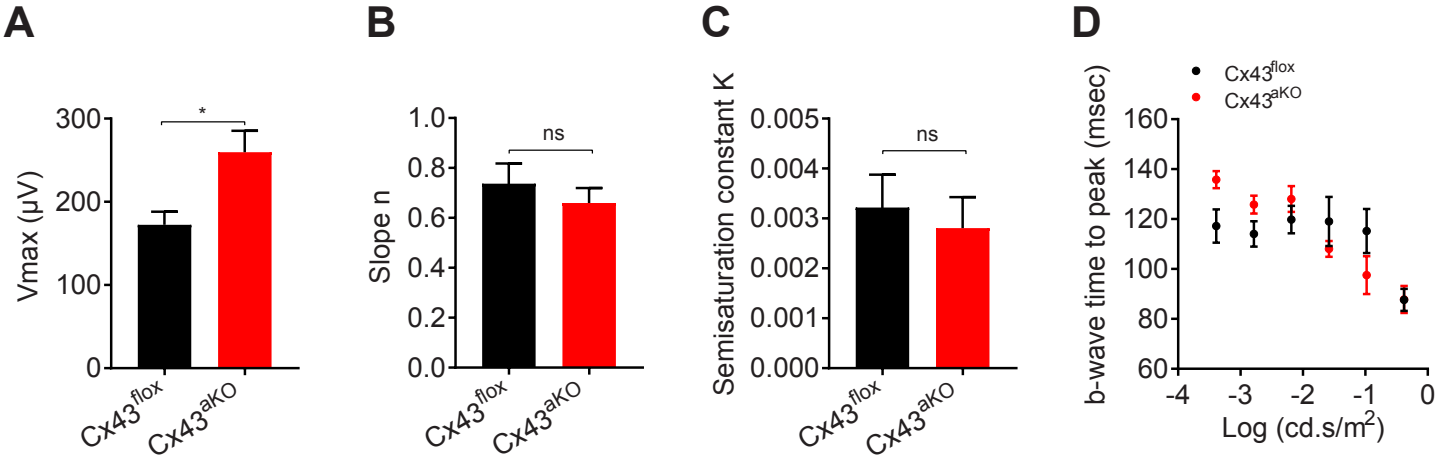

Fig. S5: Deletion of astrocytic Cx43 does not affect the slope, semisaturation constant and b-wave time-to-peak in OIR. Quantification of the maximum response amplitude (Vmax) (**A**), slope n (**B**) and semisaturation constant K (**C**) of the b-wave intensity-response function, and of the b-wave time-to-peak (**B**). Data are presented as mean ± SEM (N = 5 each of Cx43^{flox} and Cx43^{aKO} mice). Student's t test, *P < 0.05, ns > 0.05.

Fig. S6

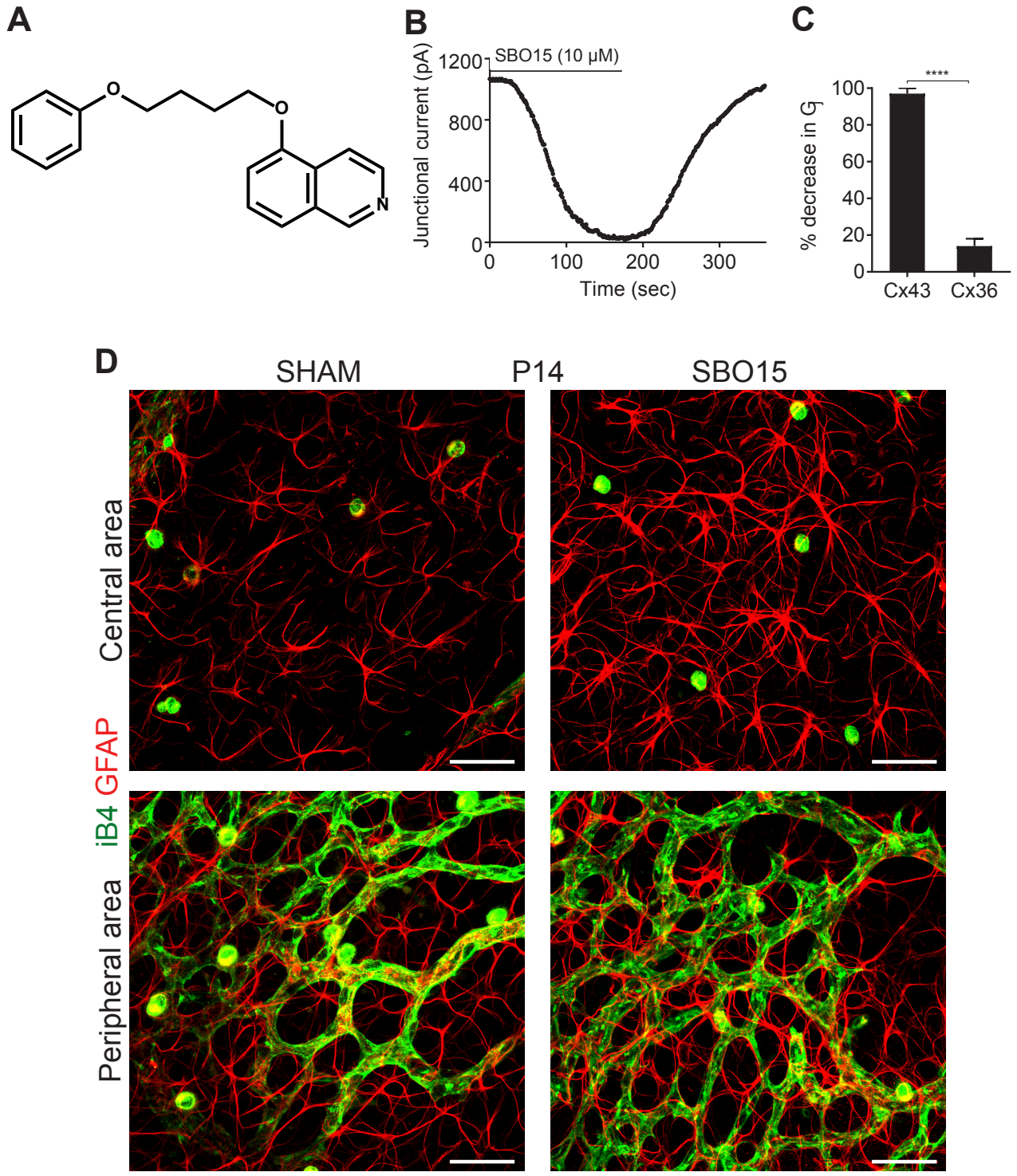

Fig. S6: **SBO15 is a selective Cx43 inhibitor.** (**A**) Structure of SBO15 (5-(4-phenoxybutoxy)isoquinoline). (**B**) Effect of SB015 (10 μM) on the junctional current in HeLa cells expressing Cx43. Junctional currents were measured in response to 200 ms pulses to −10 mV applied to one cell of a pair every 2 s from a holding potential of 0 mV. SBO15 produced a complete and reversible reduction in the junctional current. (**C**) Bar graph summarizing the effect of SBO15 (10 μM) on Cx43 GJ channels. At this concentration, SBO15 had only a modest effect on Cx36 GJ channels. Each bar represents the mean ± SEM of 4–6 cell pairs. (**D**) High magnification images from the central and peripheral retinal regions of PBS- and SBO15-injected WT retinas (shown in Figure 4D), stained with isolectin (green) and anti-GFAP (red). Scale bars: 50 μm.

Fig. S7

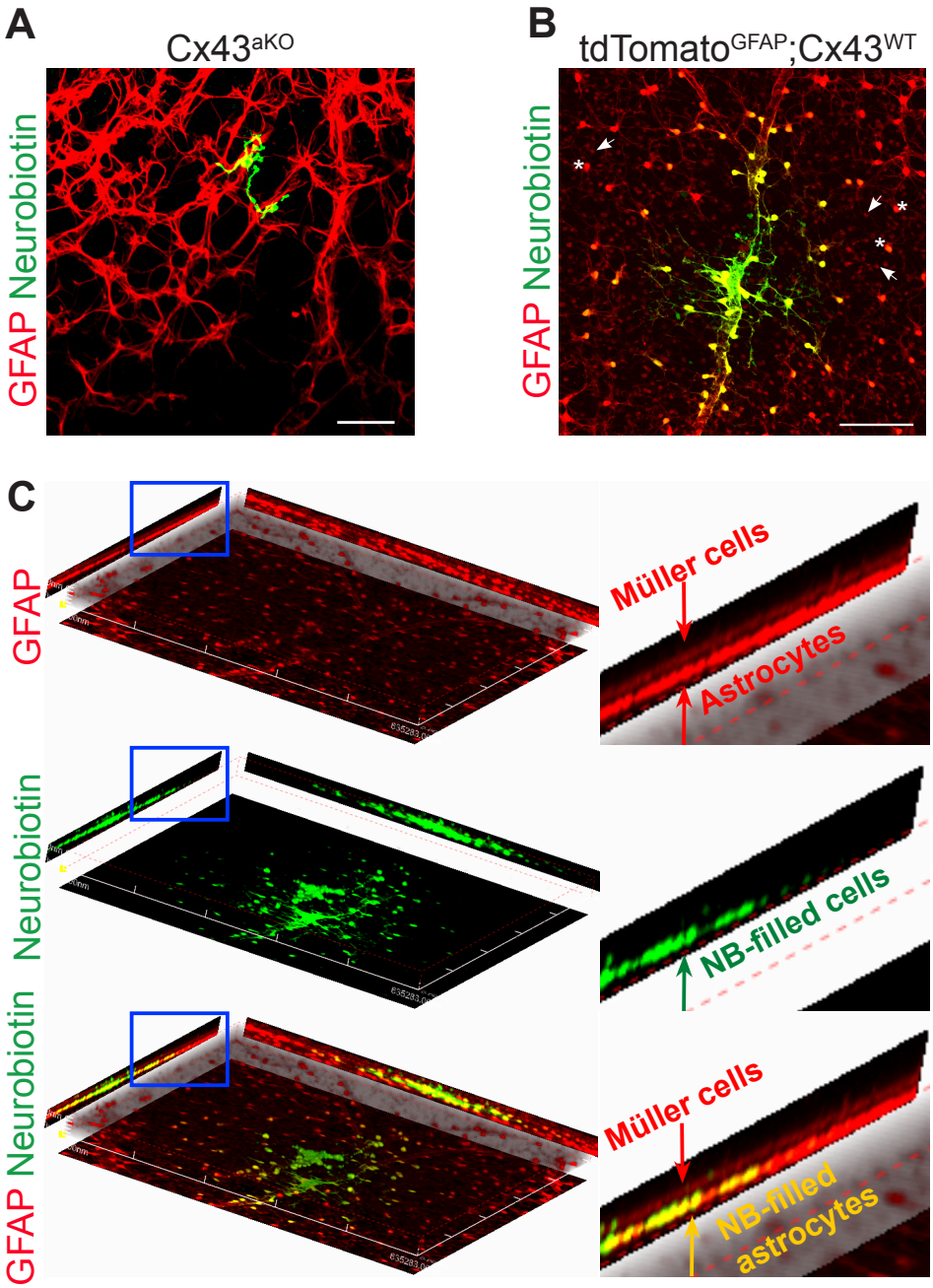

Fig. S7: **Cx43 mediates astrocyte-astrocyte but not astrocyte-Müller cell coupling.** (**A**) Streptavidin staining against Neurobiotin (green) in astrocytes (red) of a Cx43^{aKO} retina after 6 hours of hypoxia. Scale bar: 100 µm. (**B**) Z-stack (32 µm) of 20 images taken from a tdTomato^{GFAP} (Cx43^{WT}) retina loaded with Neurobiotin in one astrocyte. Yellow signal indicates overlap of Neurobiotin staining (green) with GFAP-expressing cells (red). Astrocytes (asterisks) and Müller cells (arrows) express high and low levels of GFAP, respectively. Scale bar: 200 µm. (**C**) *Left*: 3-D view of the Z-stack shown in **B**. Red and green channels are shown separately (*top* and *middle*, respectively) and merged (*bottom*). *Right*: Higher magnification of the areas in the blue boxes in the left panels. Neurobiotin loaded in astrocytes did not spread to Müller cells.

Fig. S8

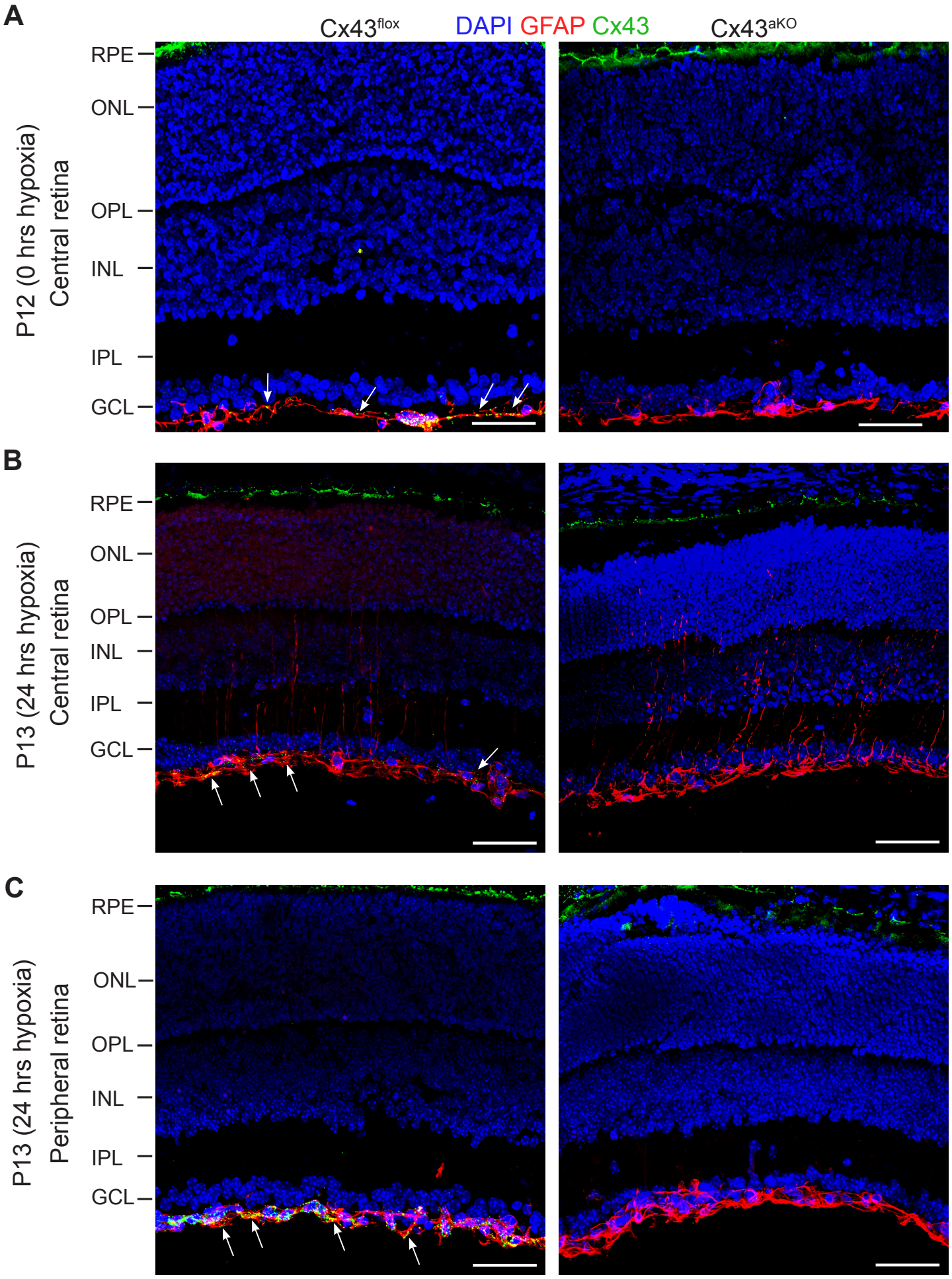
A
Cx43flox
DAPI GFAP Cx43
Cx43aKO
RPE
ONL
OPL
INL
IPL
GCL
P12 (0 hrs hypoxia)
Central retina
B
P13 (24 hrs hypoxia)
Central retina
C
P13 (24 hrs hypoxia)
Peripheral retina

Fig. S8: Expression of Cx43 in the OIR mouse retina. Representative images of vertical sections from the central regions of $Cx43^{flox}$ and $Cx43^{aKO}$ retinas after 0 hours (P12) (**A**) and 24 hours (P13) (**B**) hypoxia, or from the peripheral regions of these retinas after 24 hours (P13) hypoxia (**C**), immunostained with anti-GFAP (red) and anti-Cx43 (green). Nuclei are counterstained with DAPI (blue). Expression of GFAP in Müller cells is seen in the central, hypoxic retina but not in vascularized periphery. Reactive, GFAP-expressing Müller glia are present in the central retina after 24 hours (P13) of hypoxia, but not at 6 hours of hypoxia (P12). In both central and peripheral areas of the OIR retina, Cx43 is largely localized in the GCL, around nuclei corresponding to astrocytes (arrows) in $Cx43^{flox}$ but not $Cx43^{aKO}$ retinas. Cx43 labeling is not seen in cell bodies of Müller glia or their processes in either $Cx43^{flox}$ or $Cx43^{aKO}$ retinas. Scale bars: 50 μm.

Fig. S9

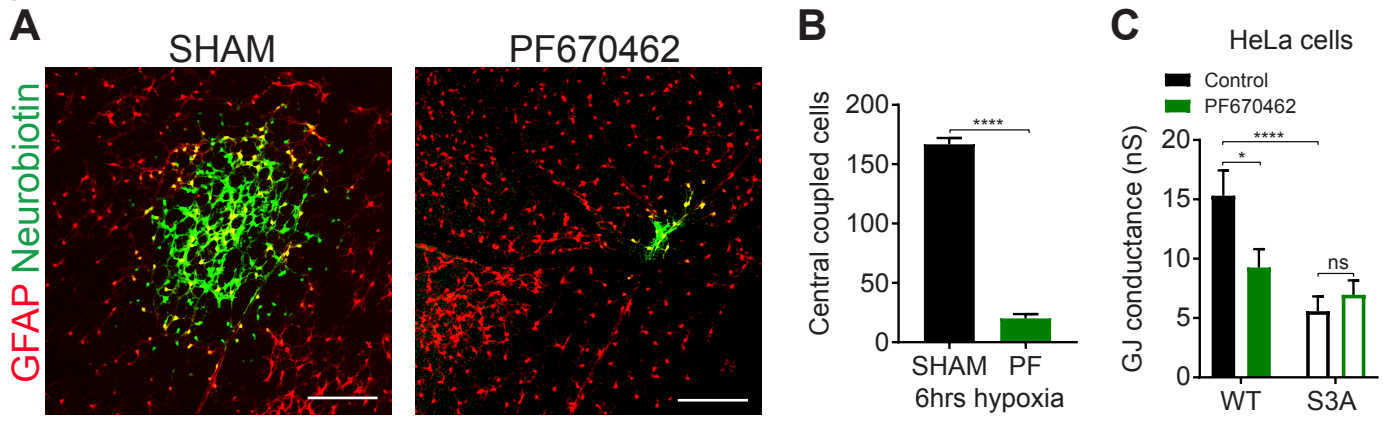

Fig. S9: **Inhibition of CK1δ reduces Cx43-mediated GJ coupling.** (**A**) Streptavidin staining against Neurobiotin (green) in astrocytes (red) of $Cx43^{WT}$ PBS-treated and PF670462-treated retinas after 6 hours of hypoxia. Scale bars: 200 μm. (**B**) Quantification of Neurobiotin-labeled astrocytes in the central areas of $Cx43^{WT}$ PBS-treated (n = 4) and PF670462-treated (n = 4) retinas after 6 hours of hypoxia. (**C**) GJ conductances measured in HeLa cells that expressed WT Cx43 or Cx43_S325A/S328A/S330A and were untreated or treated with PF670462 (n = 31-52). Data are presented as mean ± SEM. Student's t test used in **B**, Two-way ANOVA is used in **C**, ns $P > 0.05$, *$P < 0.05$, ****$P < 0.0001$.